

# Laser writing of individual nitrogen-vacancy defects in diamond with near-unity yield

YU-CHEN CHEN<sup>1,†</sup>, BENJAMIN GRIFFITHS<sup>1,2</sup>, LAIYI WENG<sup>1</sup>, SHANNON S. NICLEY<sup>1</sup>, SHAZEAA N. ISHMAEL<sup>1</sup>, YASHNA LEKHA<sup>3</sup>, SAM JOHNSON<sup>1</sup>, COLIN J. STEPHEN<sup>3</sup>, BEN L. GREEN<sup>3</sup>, GAVIN W. MORLEY<sup>3</sup>, MARK E. NEWTON<sup>3</sup>, MARTIN J. BOOTH<sup>2</sup>, PATRICK S. SALTER<sup>2</sup>, AND JASON M. SMITH<sup>1\*</sup>

<sup>1</sup>Department of Materials, University of Oxford, Parks Road, Oxford OX1 3PH, UK

<sup>2</sup>Department of Engineering Science, University of Oxford, Parks Road, Oxford OX1 3PJ, UK

<sup>3</sup>Department of Physics, University of Warwick, Coventry CV4 7AL, UK

<sup>†</sup>Current address: 3rd Institute of Physics, University of Stuttgart and Institute for Quantum Science and Technology IQST, 70550 Stuttgart, Germany

\*Corresponding author: [jason.smith@materials.ox.ac.uk](mailto:jason.smith@materials.ox.ac.uk)

Received XX Month XXXX; revised XX Month, XXXX; accepted XX Month XXXX; posted XX Month XXXX (Doc. ID XXXXX); published XX Month XXXX

Atomic defects in wide band gap materials, such as the nitrogen-vacancy (NV) color center in diamond, show considerable promise for the development of a new generation of quantum information technologies, but have been hampered by the inability to produce and engineer the defects in a controlled manner. Here we demonstrate an all-optical method for the deterministic writing of individual NV centers at selected locations with high positioning accuracy. Ultrashort pulse laser processing is used to both create and diffuse defects inside the crystal through local annealing. During the laser annealing process, online fluorescence feedback provides a trigger to stop processing once the NV formation is detected. This method provides a new tool for the optical fabrication of engineered materials and devices for quantum technologies.

© 2018 Optical Society of America

<http://dx.doi.org/10.1364/optica.99.099999>

## 1. INTRODUCTION

Color center point defects in wide band gap materials display strong optical transitions, allowing the addressing of single atoms using optical wavelengths within the transparency window of the solid. Fluorescence from single color centers displays quantum statistics with potential for use in communications, sensing and metrology [1], while some color centers also possess spin degrees of freedom that can be accessed via the optical transitions, opening the door for use as highly sensitive magnetic field sensors [2] or as quantum memories for use in optical networks for communications or computing technologies [3, 4]. To harness the technological potential of these systems, new methods in precision engineering are required for defect fabrication and manipulation.

The most extensively researched color center is the negatively charged nitrogen-vacancy (NV<sup>-</sup>) center in diamond, for which measurements on single defects were first reported by researchers at the University of Stuttgart in 1997 [5]. NV<sup>-</sup> centers have since formed a basis for advances in photon-mediated entanglement [6], quantum teleportation over long distances [7], and nanoscale nuclear magnetic

resonance [8], and are one of the few physical systems to have been shown to support quantum logic gates with fidelity above the threshold for fault-tolerant quantum computing [9].

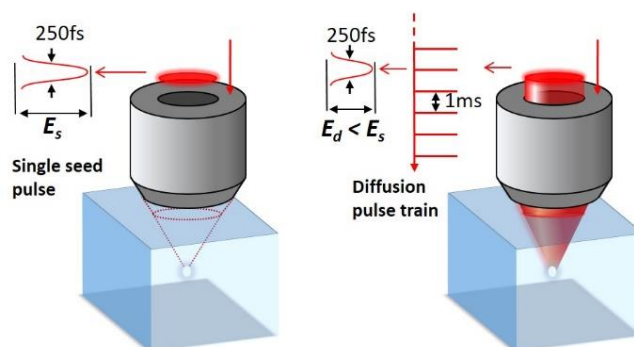


**Figure 1:** Schematic of the laser writing process. A single seed pulse is used to generate vacancies in the crystal, followed by a pulse train at lower energy to locally anneal the diamond.

NV centers are formed in diamond by the binding of a lattice vacancy with a substitutional nitrogen impurity along a [111] crystal axis. The fabrication of NV centers with controlled positioning is extremely challenging, requiring the targeted implantation of either nitrogen ions or vacancies inside the crystal. Typically, this is achieved using ion implantation and electron beam irradiation methods, followed by thermal annealing to stimulate diffusion of vacancies through the lattice whereupon random binding occurs to create the NV center [10-14]. Recently, laser processing was shown to be an effective way of writing lattice vacancies into diamond with minimal residual damage such that binding with substitutional nitrogen impurities already present in the lattice yielded high quality single NV centers [15, 16]. The ‘global’ thermal anneal used to facilitate the random diffusion of vacancies and subsequent NV center creation meant that the number of NV centers produced per site was determined by Poisson statistics such that the maximum probability of creating a single NV center at a given site was 37%. Additionally, the positioning accuracy of the resultant NV centers was determined by the vacancy diffusion length and limited to a few hundred nanometers. This low yield and modest positioning accuracy would potentially limit the usefulness of the technique in device manufacturing.

Here we report a laser writing process that allows fabrication of these atomic-scale defects with near-unity yield. We use femtosecond laser processing to not only create vacancies in the crystal but also to anneal the diamond, as illustrated by the schematic in Figure 1, providing site-specific control of NV center formation. We also employ an online fluorescence measurement that provides feedback to allow active control of the process. Due to the highly nonlinear interaction between the laser pulses and the diamond lattice, the NV centers are created with positioning accuracy significantly below the diffraction limit of fabrication laser – around 33 nm in the image plane which is a factor of 4.5 times smaller than the half-width of the focused laser spot. The ability to create single centers with purely local processing and with high yield is an important step in developing routes for the manufacturing of devices that use individual color centers as quantum light sources or qubits in quantum technologies.

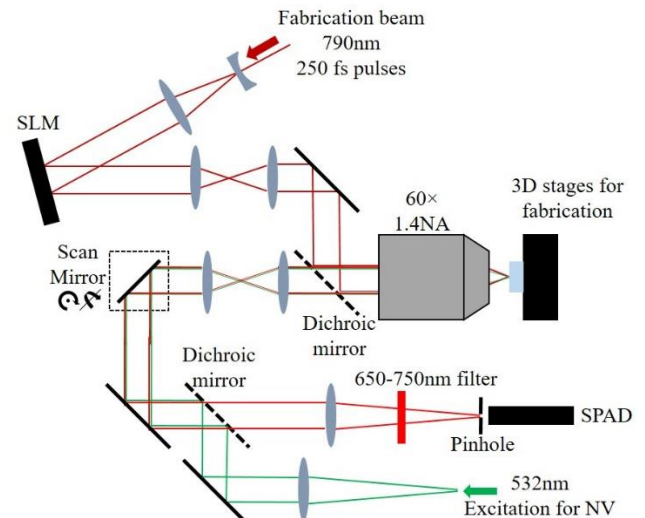
## 2. EXPERIMENTAL METHODS

Figure 2 shows a schematic diagram of the apparatus, with the laser writing system and confocal imaging system aligned through a common objective lens into a diamond sample. The laser processing was performed using an amplified Ti:Sapphire laser (Spectra Physics Solstice) at a wavelength of 790 nm and a 1 kHz pulse repetition rate. A spatial light modulator (SLM) (Hamamatsu X10468-02) was used to correct for spherical aberrations induced when the light was focused through the surface of the diamond by the high numerical aperture (NA=1.4) oil immersion objective [17]. The diamond sample was mounted on precision translation stages providing three-dimensional control with a 2.5 nm resolution and positioning repeatability specified by the manufacturer of 50 nm. Prior to the objective the laser pulse was linearly polarized and had a duration which was measured to be 250 fs using an autocorrelator. The pulse duration at focus would be slightly increased from this value due to dispersion in the objective lens.

The samples used were single-crystal type Ib diamond, produced by a High Pressure High Temperature (HPHT) technique. The samples contained 1.8 ppm of substitutional nitrogen but no pre-existing NV centers in the vicinity of the processing location. The diamond was cut and polished with flat surfaces parallel to the (110) plane of the cubic crystal.

Fluorescence feedback was measured using a custom-built scanning confocal photoluminescence (PL) microscope that was integrated into the laser writing system, as also shown in Figure 2. A dichroic mirror coupled excitation light at a wavelength of 532 nm and power 2mW into the same objective lens as used for the laser processing. Photoluminescence was collected in epi-configuration and detected after a confocal pinhole using a silicon single photon avalanche diode (Excelitas). A band-pass spectral filter transmitting wavelengths

between 650 nm and 750 nm isolated fluorescence from negatively charged NV centers, cutting out light from both the fabrication laser and Raman signal associated with the confocal excitation. The confocal microscope was aligned to the laser writing system such that it only detected fluorescence generated from the within the focal region of the fabrication laser.



**Figure 2:** The experimental system for laser writing of defects inside a crystal with fluorescence feedback

To create an NV center in the sample, initially a single laser pulse of energy 27 nJ (the ‘seed pulse’) was used to generate an ensemble of vacancies as previously reported in Ref. 15. Subsequently a 1 kHz stream of pulses of energy 19 nJ (‘annealing pulses’) irradiated the same region to induce vacancy diffusion. Fluorescence was monitored during the annealing pulse stream until a signal indicating the creation of a negatively charged NV center was recorded at which point the processing was halted.

Photon autocorrelation measurements were carried out on each laser written NV center using the Hanbury-Brown and Twiss method using single photon detecting diodes with timing resolution ~500 ps. Background signals were measured by recording the fluorescence signal from the bulk diamond misaligned from the laser writing site and were then used to calculate the baseline for the autocorrelation dataset according to the function  $a = 1 - \left(\frac{S}{S+B}\right)^2$ , where  $S$  and  $B$  are the photon count rates for the emitter and the background fluorescence, respectively. The raw datasets,  $g_{raw}^{(2)}(\tau)$ , were then corrected for this baseline according to  $g^{(2)}(\tau) = \frac{g_{raw}^{(2)}(\tau) - a}{1 - a}$ . Fluorescence spectroscopy was carried out on each site, and spectra recorded with a 500 mm spectrograph (Acton SpectraPro 500i) fitted with a back-illuminated CCD camera (Princeton Spec-10 100B). For collecting fluorescence images, a 650 nm long-pass filter was inserted in the collection path to block the diamond Raman emissions.

The position in the image plane of each single NV center could be accurately measured from the PL images since it was known that each was a single point source emitter. Thus, it was possible to determine the centroid of a 2D Gaussian surface fit to the measured intensity distribution, providing precision much higher than the intrinsic resolution of the microscope. The accuracy of the position measurements was measured to be 20 nm (standard error) by repeatedly fitting three emitters over a timescale consistent with the localization measurements (approximately 20 minutes). The target grid was determined by performing a least-squares fit of a regular rectangular grid to the PL image using fitting parameters of offset in  $x$  and  $y$ , spacing in  $x$  and  $y$ , shear and rotation to allow for systematic and

therefore correctable distortions that may have been introduced by the writing or imaging systems.

Hahn Echo measurements were performed to determine electron spin coherence times. A biasing DC magnetic field was applied parallel to the axis of the NV center within approximately  $1^\circ$  to split the  $m_s = \pm 1$  levels in the electronic ground state. A Laser Quantum Gem 532 (100 mW) was used through an Isomet 1250C acousto-optic modulator operated with a custom driver to eliminate the leakage of green laser light. The sample was mounted onto a co-planar waveguide board, and microwaves were delivered to the sample using a 20  $\mu\text{m}$  copper wire over the surface. A Keysight N5172B source was switched using a Swabian Instruments PulseStreamer and subsequently amplified with a MiniCircuits ZHL-16W-43-S+ amplifier. The spin echo signal was fitted to a stretched exponential decay function  $f(t) = e^{-(t/T_2)^\alpha}$  where  $t$  is the total free-precession time,  $T_2$  is the electron spin-coherence time and  $\alpha$  is a free-parameter related to the dynamics of the spin environment.

### 3. RESULTS

A fluorescence image of an array of 25 laser written sites on a 2  $\mu\text{m}$  square grid at a depth of 50  $\mu\text{m}$  inside the diamond is shown in Figure 3A. Measurements of fluorescence spectra and photon statistics are shown in Figure 3 B and C. The NV centers were stable in the negatively charged state with no evidence of fluorescence from the charge-neutral state  $\text{NV}^0$  (see SI Figure S6). The appearance of  $\text{NV}^0$  fluorescence was also tested for during processing by replacing the filters with a cutoff filter of all light above 650 nm whereby no fluorescence could be detected. Additionally, there was no discernible fluorescence from other defects such as the isolated vacancy (GR1) or extended defects (B band). The NV centers displayed distinct photon anti-bunching, with  $g^{(2)}(0) < 0.2$  after correction for fluorescence and Raman signals from the surrounding bulk crystal, revealing that 24 of the 25 processed sites contained a single NV center, giving a yield of 96% (see Figures S1 and S2). Figure 3D shows a typical trace of fluorescence intensity as a function of time from the online feedback during laser processing. While the sample was irradiated by the diffusion pulses, there was an intermittent fluorescent signal, which then stabilized at the higher level to indicate the formation of a stable NV center.

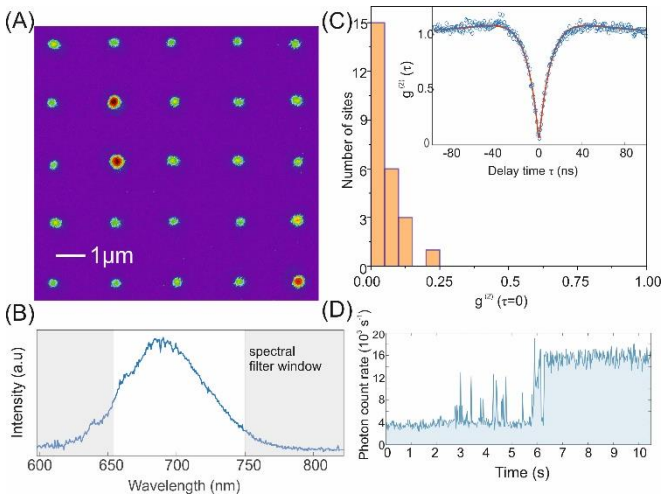


**Figure 3:** Deterministic laser writing of NV color centers in diamond. (A) Fluorescence image of a high-yield  $5 \times 5$  array of single NV centers on a 2  $\mu\text{m}$  square grid. (B) NV color center fluorescence spectrum and fluorescence monitor band. (C) Histogram of  $g^{(2)}(0)$  values for the array in (A), (inset) a typical  $g^{(2)}(\tau)$  dataset corrected for background signal from the bulk crystal. (D) Example time-trace from the fluorescence monitor. The seed pulse occurs at time = 0, and the diffusion laser pulses begin at a time of about 1 s. The onset of a stable NV signal occurs after a further 4 s. For all time traces for NVs in the array see Fig S5.

Figure 4 plots the polarization of the fluorescence from each of the defects shown in Figure 3A and fitted according to a Malus-law function as described in the supplementary information. The orientation of each NV center can be ascertained by the optical polarization of its fluorescence, since the transition dipoles of the defect lie in the plane perpendicular to the axis of threefold rotational symmetry. In the sample used, the crystal plane parallel to the surface was  $(110)$  such that NVs whose axes of symmetry were oriented along the  $[1\bar{1}1]$  and  $[\bar{1}11]$  crystal axes lay in the plane and their fluorescence displayed a high degree of linear polarization. NVs oriented along  $[111]$  and  $[1\bar{1}\bar{1}]$ , by contrast, made angles of  $55^\circ$  with the image plane, so that their fluorescence was stronger but only weakly polarized (Figure 7C). We note that the orientation of the formed defects was random, but slightly biased toward in-plane defect orientations, as will be discussed further below. The site at the right-hand end of the row second from bottom was of particular interest, as this was the only site in the array to display  $g^{(2)}(0) > 0.2$  when measuring the photon statistics. We see that the polarization of the fluorescence from the site was consistent with that from two NV defects, with different in-plane orientations, that are sufficiently close not to be resolved in the confocal microscope. When measuring the photon bunching with a linear polarization, it is thus possible to record  $g^{(2)}(0) < 0.5$ , even though a pair of NV defects are present. Thus, we conclude that from the array of 25 laser process sites, we have generated 24 single NV- centers and one double.

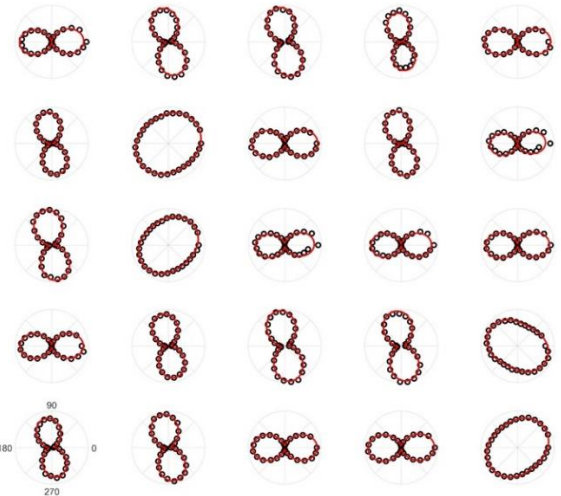


**Figure 4:** Polarization plots of fluorescence intensity revealing the orientation of the NV centers from the 25 laser processed sites shown in Figure 3A.

The exemplar trace from the fluorescence intensity monitor shown in Figure 3D shows a period of intermittent NV- fluorescence before the stable fluorescence signal is observed. This intermittent signal was an important precursor to NV- creation and an indication that the laser annealing pulses are effective in structural modification. Only a narrow window of pulse energies exists (13-19 nJ) in which the intermittent signal is detected and NV centers are generated, but continued processing does not ultimately lead to runaway lattice damage. The intermittency in the fluorescence signal prior to NV generation is tentatively interpreted as unstable binding of the vacancy to the substitutional nitrogen in the presence of strain, due to the nearby carbon split-interstitial formed as part of the Frenkel defect. A detailed explanation of the observed dynamics is the subject of ongoing investigation.

Electron spin coherence ( $T_2$ ) times were recorded using Hahn echo measurements on three example color centers as 170  $\mu\text{s}$ , 100  $\mu\text{s}$  and 10  $\mu\text{s}$ , as shown in Figure 5. This range of coherence times is likely caused by inhomogeneity in the substitutional nitrogen level and strain fields from defects, and are therefore a feature of the material used rather than



fundamental to the process. These measurements show that the process is capable of producing NV centers with coherence times long enough for quantum technology applications and that any residual damage to the local environment of the written NVs is relatively minor.

The positions of the single NV centers in the image plane relative to the targeted array points were measured with a standard error of 20 nm by establishing the centroids of the points in the fluorescence image. Figure 6A shows the spatial distribution obtained. A maximum likelihood analysis using the 2D Gaussian probability distribution  $P(\Delta x, \Delta y, \sigma) = \frac{1}{2\pi\sigma^2} e^{-(\Delta x^2 + \Delta y^2)/2\sigma^2}$  reveals a deviation parameter of  $\sigma = 39 \pm 8$  nm, indicated by the dashed circle in the figure. Quadrature subtraction of the standard error in the measurement from the measured deviation parameter revealed an in-plane deviation parameter for the fabrication technique of  $\sigma_{fab} = 33 \pm 8$  nm, a factor of 4.2 improvement over the in-plane positioning accuracy achieved in [15]. Based on the numerical aperture of the objective lens we calculate the dimensions of the laser writing focus. We find a beam waist of  $w = 297$  nm corresponding to a transverse standard deviation of 149 nm. Thus, the measured scatter in position relative to the targeted points was a factor of 4.5 times smaller than the transverse standard deviation of the writing laser focus.

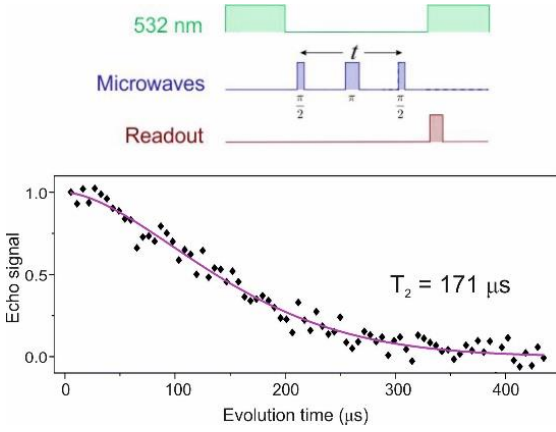


**Figure 5:** Pulse sequence for Hahn echo measurements used to record spin coherence from the laser processed NV centers shown in Figure 3A. Also shown below is data from one of the defects displaying  $T_2 = 171 \mu s$ .

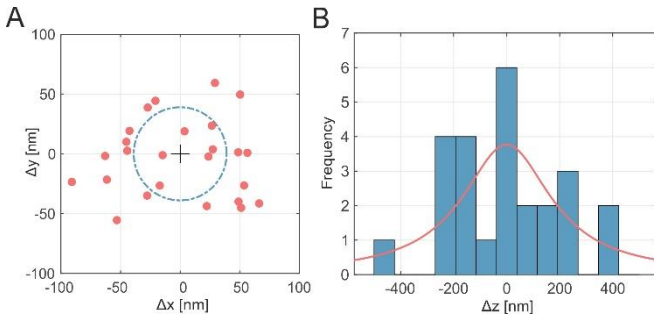


**Figure 6:** Positioning accuracy of single NV centers. (A) Scatter plot of the fitted positions of the NV centers in Figure 3A relative to the target grid in the image plane. The dashed circle represents the deviation parameter  $\sigma$  for the best fit 2D Gaussian distribution function. (B) Histogram of the fitted depths of the NV centers with a best-fit Lorentzian distribution.

The relative depth of each NV center below the sample surface was measured with an accuracy of about 50 nm from sectional fluorescence images recorded with the confocal microscope. This axial distribution was expected to be approximately Lorentzian based on the intensity distribution of the Gaussian beam near the focus. Figure 6B shows the measured distribution, together with a fitted Lorentzian line shape of half-width-at-half-maximum (HWHM)  $203 \pm 74$  nm, from which we

estimated a HWHM for the fabricated NV centers of  $197 \pm 74$  nm when the standard error for measurement was subtracted in quadrature. This depth variation is a factor of 4.3 times smaller than the calculated HWHM of the focal spot of the writing laser along the axis, the latter being equal to the Rayleigh range,  $z_R = 852$  nm.

Continued laser processing of a site beyond the creation of a single NV center can reveal rich dynamics offering additional potential for advanced device engineering. Figure 7A shows an example of a fluorescence trace in which a second NV center is formed, while Figure 7B shows a trace in which an NV center is created, then destroyed, before another defect is created at a later time. Such processes allow for a degree of selection of NV properties. The simplest example is that of NV orientation in the lattice. By terminating the annealing process when fluorescence was observed within a specific window of intensity, it was possible to exercise some control over the statistical distribution of orientations in the lattice. The array in Figure 3A was fabricated with no selection of fluorescence intensity and 23 of the 26 NV centers (88%) created were in one of the two orientations with their axes lying in the plane of the sample (Figure 7C), only three (12%) were created in the two orientations with their axes out-of-plane (the reason for this statistically significant bias is presently unknown). By terminating processing only when a signal intensity in the range 11-15 kcounts/s was observed, the fraction of NV centers created that were lying with axes out-of-plane increased to 82%. A third array in which processing was terminated when a signal of 8-11 kcounts/s was recorded revealed 84% of NV centers in the in-plane orientations (Figures 7E, S3 and S4). These results show the potential for laser writing arrays of color centers at high yield with uniform crystallographic orientation.

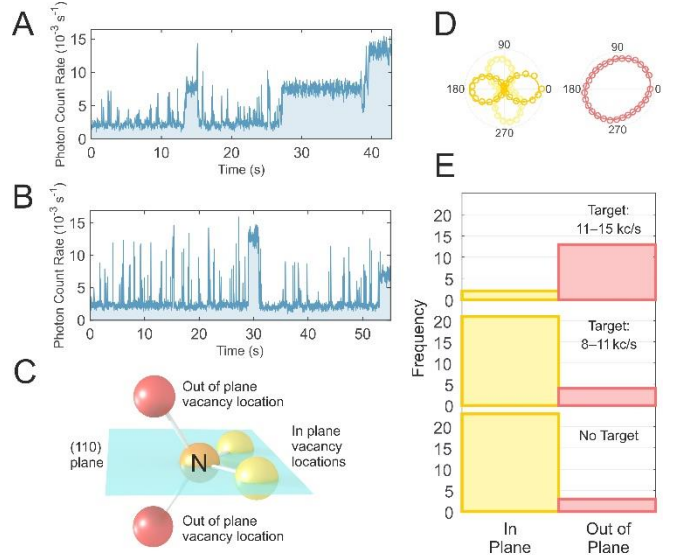


**Figure 7:** Advanced control in NV center generation. (A) Fluorescence monitor trace showing creation of two NV centers at a processing site. (B) Trace showing the creation and destruction of an NV center (time = 28 to 30 seconds) followed by selection of the second defect created. (C) Schematic of the four orientations of NV centers relative to the (110) image plane. (D) Example polarization datasets from in-plane and out-of-plane NV centers. (E) Histograms of orientations of defects in three different arrays under different termination conditions (kc = kilo counts).

## 4. DISCUSSION

The observed positioning accuracy for NV centers in this work suggests a high degree of nonlinearity in the laser processing mechanism that leads to NV formation. The generation of vacancies in diamond by a sub-picosecond laser pulse is thought to be via a sequential process of photoionization promoting electrons to high energy states, followed by rapid relaxation of the electrons by transfer of their energy to the lattice, and it is reasonable to assume that vacancy diffusion occurs by a similar process. A detailed study of the

photoionization of diamond by Ti:Sapphire laser pulses of 30 fs duration has been presented by Lagomarsino *et al* [18] showing that this process is highly non-linear, with multiphoton absorption beyond that of the number of photons required to traverse the band-gap. Vacancy generation is indirect, through the relaxation of hot electrons, however, it is expected to exhibit a substantially higher nonlinearity based on the minimum energy required to create a Frenkel defect of 30 eV [19]. Vacancy diffusion, by contrast, has a relatively low activation energy of 2.3 eV [20] such that the relaxation of photoionized electrons even at relatively low pulse energies would release sufficient energy to move a vacancy to an adjacent lattice site. The diffusion of carbon self-interstitials, with an activation energy of 1.6 eV [21], is also expected to be activated by low energy laser pulses. NV formation requires a vacancy to first be generated and then to hop multiple times before it binds stably to a nitrogen atom, resulting in a large cumulative nonlinearity. We note that these observations contrast with recent work by Kononenko *et al.* which revealed a logarithmic dependence of NV generation over a wide range of laser fluence during nanoablation of the diamond surface [22].

## 5. CONCLUSION

In summary, we have reported a method for localized laser processing of wide band gap materials with fluorescence feedback and demonstrated the near-deterministic creation of single NV centers at desired locations in diamond. Feedback provided by online monitoring may be used to provide information on defect formation, and to identify a range of other properties of the color centers created, providing additional routes to device engineering.

The positioning accuracy for NV center creation demonstrated with this method is a factor of 4.5 higher than the diffraction-limited spatial resolution of the optical microscope, due to the highly nonlinear interaction of the laser pulse with the diamond lattice. The in-plane accuracy of 33 nm, if combined with improved depth positioning using delta doping of nitrogen impurities, is sufficient to facilitate high yield positioning within photonic crystal waveguides or microcavities, or to produce pairs or small groups of NV centers close enough to interact via magnetic dipolar coupling of their electron spins.

The processing method can in principle be applied to the controlled writing of other color centers in diamond, or fluorescent defects in other materials such as recently reported demonstrations of laser written color centers in silicon carbide [23, 24], cubic boron nitride [25] or gallium nitride [26]. Its range of applicability will however depend on the production of materials with highly engineered doping, such that the impurities needed for formation of vacancy complexes are present at appropriate concentrations and with existing complexes at acceptably low levels. The technique is straightforward to implement with other aspects of subsurface laser writing in crystals [27-29] and can provide a tool with potential for wide application in the engineering of materials at the quantum level.

**Funding.** Engineering and Physical Sciences Research Council (EPSRC) (EP/M013243/1, EP/R004803/1); The Royal Society; The Royal Academy of Engineering.

**Acknowledgment.** We thank DeBeers and Element Six for providing suitably characterized diamond samples for this work, and in particular David Fisher and Daniel Twitchen for helpful comments.

See [Supplementary Information](#) for supporting content.

## REFERENCES

1. B. Lounis and M. Orrit, "Single-photon sources," *Rep. Prog. Phys.* 68, 1129-1179 (2005).
2. L. Rondin, J.-P. Tetienne, T. Hingant, J.-F. Roch, P. Maletinsky, and V. Jacques, "Magnetometry with nitrogen-vacancy defects in diamond," *Rep. Prog. Phys.* 77, 056503 (2014).
3. C. Simon, M. Afzelius, J. Appel, A. Boyer de la Giroday, S. J. Dewhurst, N. Gisin, C. Y. Hu, F. Jelezko, S. Kröll, J. H. Müller, J. Nunn, E. S. Polzik, J. G. Rarity, H. De Riedmatten, W. Rosenfeld, A. J. Shields, N. Sköld, R. M. Stevenson, R. Thew, I. A. Walmsley, M. C. Weber, H. Weinfurter, J. Wrachtrup, and R. J. Young, "Quantum Memories," *Eur. Phys. J. D* 58, 1-22 (2010).
4. F. Jelezko, T. Gaebel, I. Popa, M. Domhan, A. Gruber, and J. Wrachtrup, "Observation of Coherent Oscillation of a Single Nuclear Spin and Realization of a Two-Qubit Conditional Quantum Gate," *Phys. Rev. Lett.* 93, 130501 (2004).
5. A. Gruber, A. Dräbenstedt, C. Tietz, L. Fleury, J. Wrachtrup and C. von Borczyskowski, "Scanning Confocal Optical Microscopy and Magnetic Resonance on Single Defect Centers," *Science* 276, 2012-2014 (1997).
6. B. Hensen, H. Bernien, A. E. Dréau, A. Reiserer, N. Kalb, M. S. Blok, J. Ruitenbergh, R. F. L. Vermeulen, R. N. Schouten, C. Abellán, W. Amaya, V. Pruneri, M. W. Mitchell, M. Markham, D. J. Twitchen, D. Elkouss, S. Wehner, T. H. Taminiau and R. Hanson, "Loophole-free Bell inequality violation using electron spins separated by 1.3 kilometres," *Nature* 526, 682-686 (2015).
7. W. Pfaff, B. J. Hensen, H. Bernien, S. B. van Dam, M. S. Blok, T. H. Taminiau, M. J. Tiggelman, R. N. Schouten, M. Markham, D. J. Twitchen, and R. Hanson, "Unconditional quantum teleportation between distant solid-state quantum bits," *Science* 345, 532-535 (2014).
8. H. J. Mamin, M. Kim, M. H. Sherwood, C. T. Rettner, K. Ohno, D. D. Awschalom, and D. Rugar, "Nanoscale nuclear magnetic resonance with a nitrogen-vacancy spin sensor," *Science* 339, 557-560 (2013).
9. X. Rong, J. Geng, F. Shi, Y. Liu, K. Xu, W. Ma, F. Kong, Z. Jiang, Y. Wu & J. Du, "Experimental fault-tolerant universal quantum gates with solid-state spins under ambient conditions," *Nature Commun.* 6, 8748 (2015).
10. J. Meijer, B. Burchard, M. Domhan, C. Wittmann, T. Gaebel, I. Popa, F. Jelezko, and J. Wrachtrup, "Generation of single colour centers by focussed nitrogen implantation," *Appl. Phys. Lett.* 87, 261909 (2005).
11. J. Rabeau, P. Reichart, G. Tamanyan, D. N. Jamieson, S. Praver, F. Jelezko, T. Gaebel, I. Popa, M. Domhan, and J. Wrachtrup, "Implantation of labelled single nitrogen vacancy centers in diamond using  $^{15}\text{N}$ ," *Appl. Phys. Lett.* 88, 023113 (2006).
12. D. M. Toyli, C. D. Weis, G. D. Fuchs, T. Schenkel and D. D. Awschalom, "Chip-Scale Nanofabrication of Single Spins and Spin Arrays in Diamond," *Nano Lett.* 10, 3168-3172 (2010).
13. C. A. McLellan, B. A. Myers, S. Kraemer, K. Ohno, D. D. Awschalom, and A. C. Bleszynski Jayich, "Patterned Formation of Highly Coherent Nitrogen-Vacancy Centers Using a Focused Electron Irradiation Technique," *Nano Lett.* 16, 2450-2454 (2016).
14. D. Scarabelli, M. Trusheim, O. Gaathon, D. Englund, and S. J. Wind, "Nanoscale Engineering of Closely-Spaced Electronic Spins in Diamond," *Nano Lett.* 16, 4982-4990 (2016).
15. Y.-C. Chen, P. S. Salter, S. Knauer, L. Weng, A. C. Frangeskou, C. J. Stephen, S. N. Ishmael, P. R. Dolan, S. Johnson, B. L. Green, G. W. Morley, M. E. Newton, J. G. Rarity, M. J. Booth, and J. M. Smith, "Laser writing of coherent colour centers in diamond," *Nature Photon.* 11, 77-80 (2017).
16. C. J. Stephen, B. L. Green, Y. N. D. Lekhai, L. Weng, P. Hill, S. Johnson, A. C. Frangeskou, P. L. Diggle, M. J. Strain, E. Gu, M. E. Newton, J. M. Smith, P. S. Salter, G. W. Morley, "Three-dimensional solid-state qubit arrays with long-lived spin coherence," *arXiv:1807.03643*.
17. R. D. Simmonds, P. S. Salter, A. Jesacher, and M. J. Booth, "Three dimensional laser microfabrication in diamond using a dual adaptive optics system," *Opt. Express* 19, 24122-24128 (2011).
18. S. Lagomarsino, S. Sciortino, B. Obreshkov, T. Apostolova, C. Corsi, M. Bellini, E. Berdermann, and C. J. Schmidt, "Photoionization of monocrystalline CVD diamond irradiated with ultrashort intense laser pulse," *Phys. Rev. B* 93, 085128 (2016).
19. D. Delgado and R. Vila, "Statistical Molecular Dynamics study of displacement energies in diamond," *J. Nuclear Mater.* 419, 32 (2011).
20. G. Davies, S. C. Lawson, A. T. Collins, A. Mainwood, and S. J. Sharp, "Vacancy-related centers in diamond," *Phys. Rev. B* 46, 13157 (1992).
21. D. J. Twitchen, D. J. Twitchen, D. C. Hunt, C. Wade, M. E. Newton, J. M. Baker, T. R. Anthony and W. F. Banholzer "The production and annealing stages of the self-interstitial (R2) defect in diamond," *Physica B* 273, 644 (1999).

22. V. V. Kononenko, I. I. Vlasov, V. M. Gololobov, T. V. Kononenko, T. A. Semenov, A. A. Khomich, V. A. Shershulin, V. S. Krivobok, and V. I. Konov, "Nitrogen-vacancy defects in diamond produced by femtosecond laser nanoablation technique," *Appl. Phys. Lett.* 111, 081101 (2017).
23. S. Castelletto A. F. M. Almutairi, K. Kumagai, T. Katkus, Y. Hayasaki, B. C. Johnson, and S. Juodkazis, "Photoluminescence in hexagonal silicon carbide by direct femtosecond laser writing," *Opt. Lett.* 43, 6077-6080 (2018)
24. Y.-C. Chen, P. S. Salter, M. Niethammer, M. Widmann, F. Kaiser, R. Nagy, N. Morioka, C. Babin, J. Erlekampf, P. Berwian, M. Booth, and J. Wrachtrup, "Laser writing of scalable single colour centre in silicon carbide," *arXiv:1812.04284* (2018).
25. R. Buividas, I. Aharonovich, G. Seniutinas, X. W. Wang, L. Rapp, A. V. Rode, T. Taniguchi, and S. Juodkazis, "Photoluminescence from voids created by femtosecond-laser pulses inside cubic-BN," *Opt. Lett.* 40, 5711-5713 (2016).
26. U. Saleem, M. D. Birowosuto, S. Hou, A. Maurice, T. B. Kang, E. H. T. Teo, M. Tchernycheva, N. Gogneau, and H. Wang, "Light emission from localised point defects induced in GaN crystal by a femtosecond-pulsed laser," *Opt. Mater. Express* 8, 2703-2712 (2018).
27. A. Courvoisier, M. J. Booth, and P. S. Salter, "Inscription of 3D waveguides in diamond using an ultrafast laser," *Appl. Phys. Lett.* 109, 031109 (2016).
28. B. Sotillo, V. Bharadwaj, J. P. Hadden, M. Sakakura, A. Chiappini, T. T. Fernandez, S. Longhi, O. Jedrkiewicz, Y. Shimotsuma, L. Criante, R. Osellame, G. Galzerano, M. Ferrari, K. Miura, R. Ramponi, P. E. Barclay, and S. M. Eaton, "Diamond photonics platform enabled by femtosecond laser writing," *Sci. Rep.* 6, 35566 (2016).
29. J. P. Hadden, V. Bharadwaj, B. Sotillo, S. Rampini, R. Osellame, J. D. Witmer, H. Jayakumar, T. T. Fernandez, A. Chiappini, C. Armellini, M. Ferrari, R. Ramponi, P. E. Barclay, and S. M. Eaton, "Integrated waveguides and deterministically positioned nitrogen vacancy centers in diamond created by femtosecond laser writing," *Opt. Lett.* 43, 3586-3589 (2018).